MDPI

Article

Temperature- and Frequency-Dependent Ferroelectric Characteristics of Metal-Ferroelectric-Metal Capacitors with Atomic-Layer-Deposited Undoped HfO_2 Films

Chan-Hee Jang [1], Hyun-Seop Kim [1,2], Hyungtak Kim [1] and Ho-Young Cha [1,*]

[1] School of Electrical and Electronic Engineering, Hongik University, 94 Wausan-ro, Mapo-gu, Seoul 04066, Korea; chanhee7208@g.hongik.ac.kr (C.-H.J.); hyunseop.kim@bristol.ac.uk (H.-S.K.); hkim@hongik.ac.kr (H.K.)

[2] Center for Device Thermography and Reliability (CDTR), University of Bristol, Bristol BS8 1TL, UK

* Correspondence: hcha@hongik.ac.kr; Tel.: +82-2-320-3062

Abstract: In this study, we evaluated the temperature- and frequency-dependent ferroelectric characteristics of TiN/undoped HfO_2/TiN metal-ferroelectric-metal (MFM) capacitors in which an undoped HfO_2 film was deposited through atomic layer deposition (ALD). Successful ferroelectric characteristics were achieved after postdeposition annealing at 650 °C, which exhibited a remanent polarization of 8 $\mu C/cm^2$ and a coercive electric field of 1.6 MV/cm at 25 °C (room temperature). The ferroelectric property was maintained at 200 °C and decreased as the temperature increased. The ferroelectric property was completely lost above 320 °C and fully recovered after cooling. The frequency dependency was evaluated by bias-dependent capacitance–voltage and s-parameter measurements, which indicated that the ferroelectric property was maintained up to several hundred MHz. This study reveals the ultimate limitations of the application of an undoped HfO_2 MFM capacitor.

Keywords: ferroelectric; undoped HfO_2; metal-ferroelectric-metal; temperature; frequency; atomic layer deposition

Citation: Jang, C.-H.; Kim, H.-S.; Kim, H.; Cha, H.-Y. Temperature- and Frequency-Dependent Ferroelectric Characteristics of Metal-Ferroelectric-Metal Capacitors with Atomic-Layer-Deposited Undoped HfO_2 Films. *Materials* **2022**, *15*, 2097. https://doi.org/10.3390/ma15062097

Academic Editors: Lukasz Wachnicki and Sylwia Gierałtowska

Received: 10 February 2022
Accepted: 8 March 2022
Published: 12 March 2022

Publisher's Note: MDPI stays neutral with regard to jurisdictional claims in published maps and institutional affiliations.

Copyright: © 2022 by the authors. Licensee MDPI, Basel, Switzerland. This article is an open access article distributed under the terms and conditions of the Creative Commons Attribution (CC BY) license (https://creativecommons.org/licenses/by/4.0/).

1. Introduction

Ferroelectric thin films have promising potential for various applications, including nonvolatile memories, energy-related devices, and negative capacitance field-effect transistors [1–5]. Although various ferroelectric materials, such as P(VDF-TrFE), Pb(Zr,Ti)O_3 (PZT), and $BaTiO_3$, have previously been intensively studied [2,5–9], HfO_2 thin films have received significant attention recently owing to their excellent properties, such as high dielectric constant (20–25) and wide energy bandgap (~5.68 eV). Moreover, HfO_2 thin films can be deposited using a complementary metal–oxide–semiconductor (CMOS) compatible atomic layer deposition (ALD) process [10–14]. Because ALD is based on self-limiting reactions leading to layer-by-layer growth, it exhibits a large-area uniformity and significant conformability, offering atomic-scale controllability [15]. The ferroelectric properties of HfO_2 thin films have been reported with doping processes using various dopant elements, such as ZrO, Gd, Si, Al, Y, Sr, and La [4,5,16–19]. It has also been reported that the ferroelectric property can be achieved in undoped HfO_2 films without the doping process [20–23]. Considering the deposition process, ALD doped HfO_2 films require a higher deposition temperature than undoped HfO_2 films to achieve the ferroelectric property [12,24]. Therefore, undoped HfO_2 films have advantages of a lower temperature process and easy implementation without a delicate doping process [12,24,25].

Because of the mechanical dipole moment of ferroelectric materials, it is useful to determine the maximum temperature and frequency ranges to maintain the ferroelectric property of the MFM capacitor. Although various studies have been reported for different ferroelectric materials in a limited range of temperature and frequency [3,25–32], no study

has been conducted with a MFM capacitor based on undoped HfO_2. In this study, the ferroelectric property of an ALD-deposited undoped HfO_2 thin film was successfully achieved via a postdeposition annealing process. Temperature-dependent polarization and frequency-dependent capacitance characteristics were measured up to >300 °C and GHz range, respectively, to determine the fundamental limitations of the ferroelectricity of TiN/undoped HfO_2/TiN MFM capacitors.

2. Device Structure and Fabrication

TiN/undoped HfO_2/TiN MFM capacitors were fabricated on a quartz substrate to eliminate the dielectric loss during high-frequency measurements. TiN electrodes play an important role in undoped HfO_2 films. Unlike doped HfO_2 films, the N impurity provided by metal nitrides is responsible for achieving the ferroelectric properties of undoped HfO_2 films [33]. Figure 1a,b shows the top and cross-sectional schematics of the MFM capacitor, respectively, where a ground–signal–ground (GSG) pattern was employed for the s-parameter measurement.

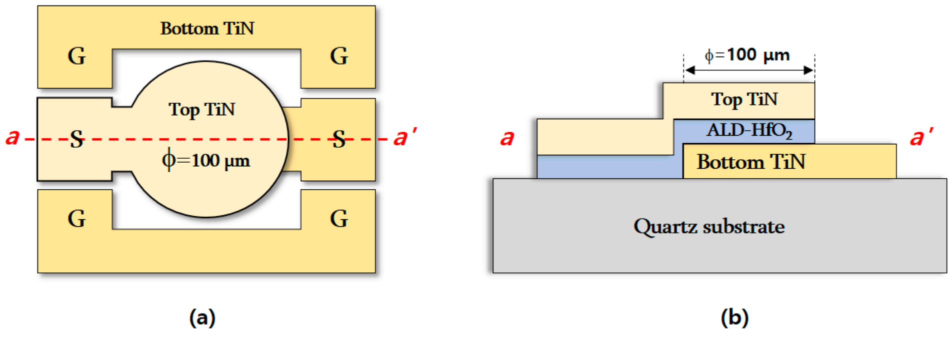

Figure 1. (**a**) Top view and (**b**) cross-sectional schematic along *a*–*a*′ of TiN/undoped HfO_2/TiN MFM capacitor fabricated on a quartz substrate.

The fabrication process of the device was as follows. After cleaning the substrates, a TiN bottom electrode with a thickness of 100 nm was deposited via RF sputtering. The films were deposited at a process pressure of 1 mTorr and an RF power of 600 W in Ar/N_2 (10/25 sccm) ambient at two different temperatures, namely 25 °C (room temperature) and 250 °C. The sheet resistance of the TiN films deposited at room temperature and 250 °C were 9.89 and 9.33 Ω/sq, respectively. After patterning the bottom electrode, the TiN layer was etched using a fluorine-based plasma etching process. A 10 nm thick undoped HfO_2 film was deposited via ALD at 220 °C with a TEMA-Hf precursor and O_3 at a concentration of 100 gm^{-3}. The deposition cycle consisted of a TEMA-Hf pulse time of 1 s, purge time of 20 s, O_3 pulse time of 0.5 s, and purge time of 15 s. The growth per cycle was 1 Å/cycle, and the refractive index (RI) was 2.01. A TiN top electrode with a thickness of 100 nm was deposited on the undoped HfO_2 film using RF sputtering. The top electrode was patterned and etched to complete the device structure. The diameter of the active region of the MFM capacitor was 100 μm. The fabricated MFM capacitors were annealed via rapid thermal annealing (RTA) at 650 °C for 1 min in a N_2 atmosphere to achieve ferroelectric property. It was observed in our previous experiments that the optimum RTA temperature was 650 °C; the ferroelectric property was slightly weaker with RTA at 600 °C and noticeably reduced with RTA at 700 °C.

3. Results and Discussion

3.1. Ferroelectric Characteristics of TiN/Undoped HfO_2/TiN MFM Capacitor

The polarization–electric field (P–E) characteristics of fabricated TiN/undoped HfO_2/TiN MFM capacitors measured at 100 kHz before and after RTA are shown in Figure 2a,b, respectively. Although no hysteresis in the P–E characteristics was observed before RTA, successful ferroelectric property was achieved after RTA. No significant differ-

ence was observed in the P–E characteristics as a function of the deposition temperature for the TiN electrodes. When both the top and bottom electrodes were deposited at room temperature, the remanent polarization (P_r) was 6.8 μC/cm^2, and the coercive field (E_c) was 1.46 MV/cm. When the electrodes were deposited at 250 °C, the values slightly decreased: P_r = 6.15 μC/cm^2 and E_c = 1.2 MV/cm.

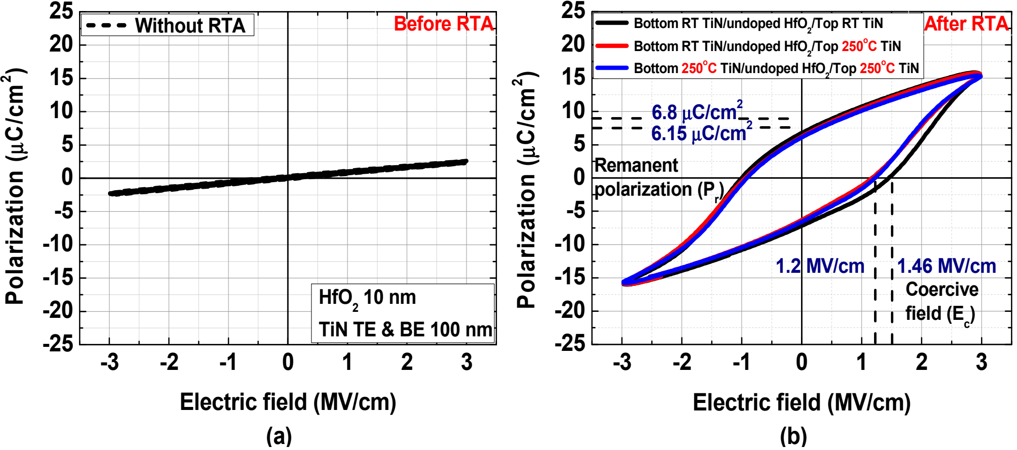

Figure 2. Polarization–electric field (P–E) characteristics of TiN/undoped HfO_2/TiN MFM capacitors before (**a**) and after (**b**) RTA with different TiN deposition temperature conditions.

The permittivity–voltage characteristics of fabricated MFM capacitors were derived from the capacitance–voltage (C–V) characteristics measured at different frequencies. Figure 3 shows the frequency-dependent permittivity versus voltage characteristics for different samples; Figure 3d compares the maximum permittivity values as a function of the measurement frequency. The permittivity decreased as the frequency increased for all samples. The permittivity is determined by free dipoles oscillating in the presence of an alternating electric field. As the frequency increases, the dipoles begin to lag behind the electric field change, which decreases the permittivity [32]. As shown in Figure 3, the MFM capacitor with only the top electrode deposited at 250 °C exhibited relatively higher permittivity over the entire range of frequencies evaluated in this study. We speculate that the difference in permittivity was associated with unbalanced strains caused by the bottom and top TiN electrodes. Figure 4a,b shows the grazing-angle incident X-ray diffraction (GIXRD) patterns measured for two samples prepared with different TiN electrode deposition temperatures of room temperature and 250 °C, respectively. It was observed that a TiN (111) peak was dominant for the sample deposited at room temperature, whereas a TiN (200) peak was dominant for the sample deposited at 250 °C. Because of the different grain sizes and strains between TiN (111) and TiN (200) [34], the HfO_2 film experienced unbalanced strains when the top TiN electrode was deposited at 250 °C, whereas the bottom TiN electrode was deposited at room temperature, which was responsible for the higher permittivity. It was reported that the strain increased the permittivity of the dielectric thin films [35,36]. It should be noted that new peaks appeared after the RTA process for both samples, which corresponded to the noncentrosymmetric o-phases that are responsible for the ferroelectric property [37].

The MFM capacitor with the bottom electrode deposited at room temperature and the top electrode deposited at 250 °C was chosen for the following study.

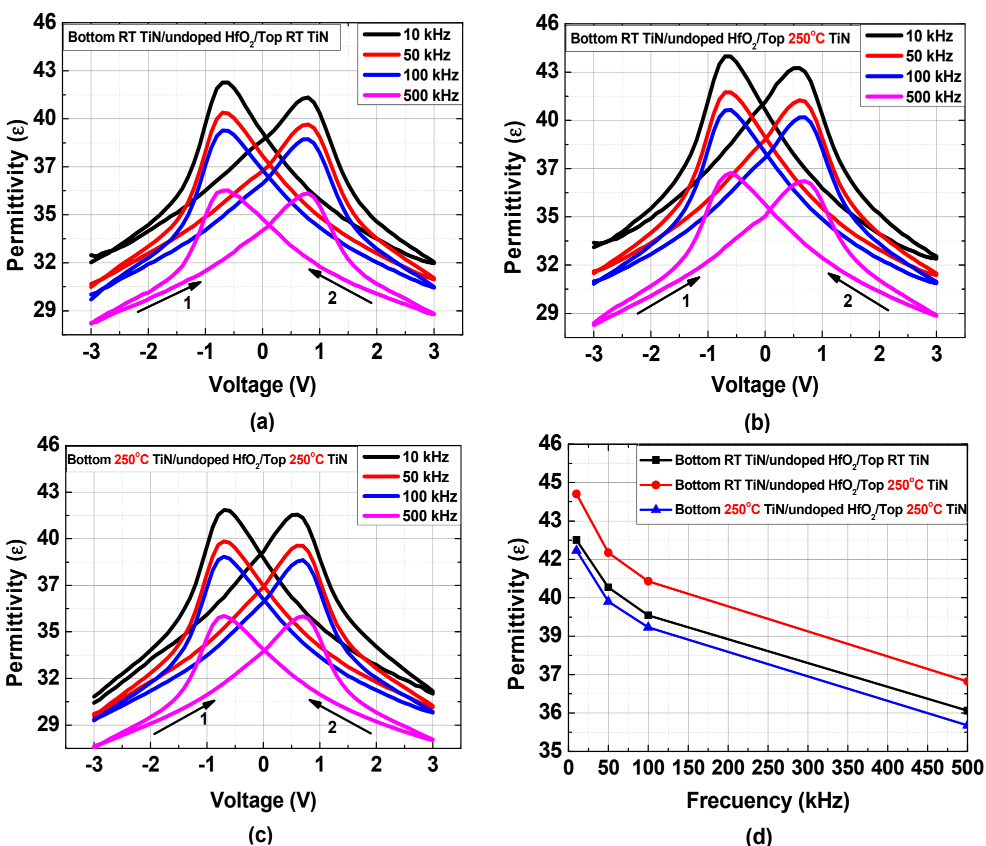

Figure 3. Frequency–dependent permittivity–voltage characteristics of MFM capacitors fabricated with different deposition temperatures for TiN electrodes. (**a**) Top and bottom electrodes deposited at room temperature, (**b**) bottom electrode at room temperature and top electrode at 250 °C, and (**c**) top and bottom electrodes at 250 °C. (**d**) Comparison of the maximum permittivity values for devices (**a**–**c**) as a function of measurement frequency.

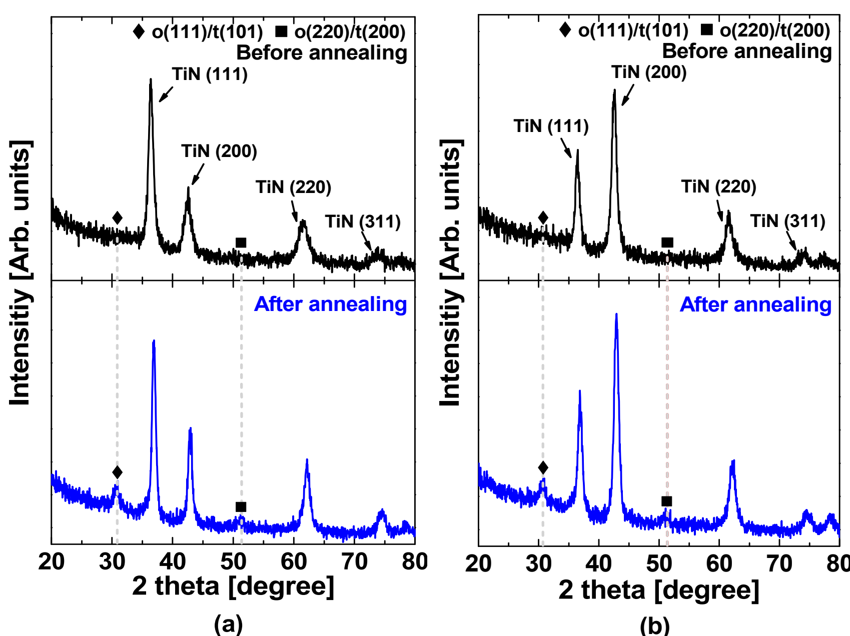

Figure 4. GIXRD patterns measured before and after the RTA process for TiN/undoped HfO_2/TiN samples with both top and bottom TiN electrodes deposited at (**a**) room temperature and (**b**) 250 °C.

3.2. Temperature-Dependent Ferroelectric Property of TiN/Undoped HfO$_2$/TiN MFM Capacitor

The temperature-dependent P–E characteristics of the MFM capacitor were evaluated in the temperature range from room temperature to 320 °C. As shown in Figure 4a, the ferroelectric hysteresis was maintained at 150 °C with a slight decrease in E_c and a slight increase in the saturation polarization (P_s). The increased P_s is owing to the relaxation of oxygen vacancies, which can significantly contribute to their recombination, improving the ferroelectricity of the HfO_2 film [28]. As shown in Figure 5a–c, significant deformation in the polarization characteristics occurred at 200 °C and significant degradation was observed at higher temperatures. The decreased P_r value at 200 °C is attributed to weaker spontaneous polarization caused by partial transition from the ferroelectric phase to the antiferroelectric phase and/or more defect formation at higher temperatures [28]. The hysteresis disappeared at temperatures higher than ~310 °C. Notably, this is the highest temperature at which an HfO_2 MFM capacitor exhibits ferroelectric properties, although special composite materials, such as $BaTiO_3$:Sm_2O_3, can achieve even higher operation temperature [3,28–31,38,39].

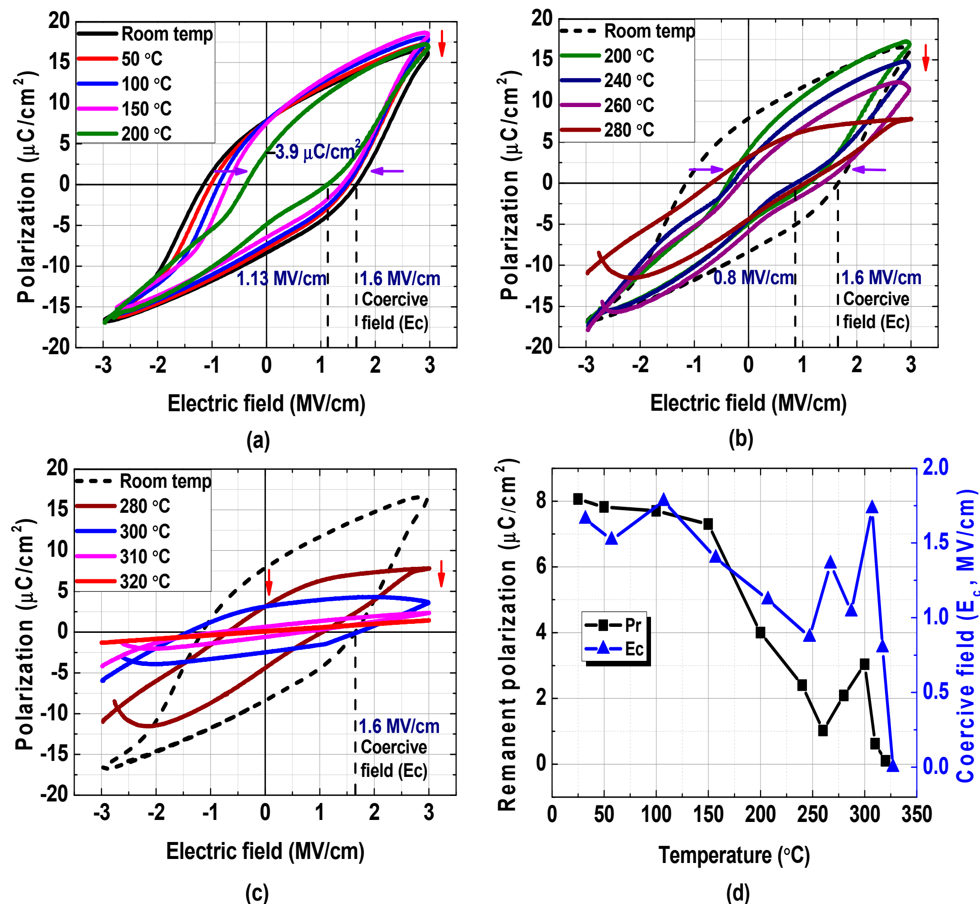

Figure 5. P–E characteristics of fabricated TiN/undoped HfO_2/TiN MFM capacitor as a function of temperature: (**a**) from room temperature to 200 °C, (**b**) from 200 °C to 280 °C, and (**c**) from 280 °C to 320 °C. (**d**) P_r and E_c as functions of temperature.

3.3. Frequency-Dependent Ferroelectric Characteristics of TiN/Undoped HfO$_2$/TiN MFM Capacitor

To determine the frequency-dependent ferroelectric property of the fabricated MFM capacitor, C–V and s-parameter measurements were employed. The butterfly-shaped capacitance characteristics were measured at frequencies ranging from 10 kHz to 1 MHz, as shown in Figure 6a. The maximum capacitance value (C_{MAX}) was obtained at a bias voltage of −0.5 V, whereas the minimum capacitance value (C_{MIN}) was obtained at −3 V,

and the capacitance tunability was defined by $C_{MAX} - C_{MIN}$ [25]. Because conventional C–V measurements cannot be used at very high frequencies, the equivalent circuit of the MFM capacitor was extracted by s-parameter measurements; for high frequencies, it is convenient to describe a given network in terms of waves rather than voltages or currents [40]. The s-parameter measurements for the GSG pattern were performed in a frequency ranging from 100 MHz to 10 GHz using a network analyzer with the bias voltage conditions obtained for C_{MAX} and C_{MIN} at C–V measurements. The GSG-type MFM structure shown in Figure 1a can be modeled as capacitors connected in series, and the intrinsic ferroelectric capacitance can be extracted by converting the s-parameter into ABCD parameters [25,27]. Z_o in Equation (1) was 50 Ω in the s-parameter measurement.

$$\text{Capacitance} = \frac{1}{j\omega \times \text{imag}(B)},\ \text{where } B = Z_o \frac{(1+S_{11})(1+S_{22}) - S_{12}S_{21}}{2S_{21}} \quad (1)$$

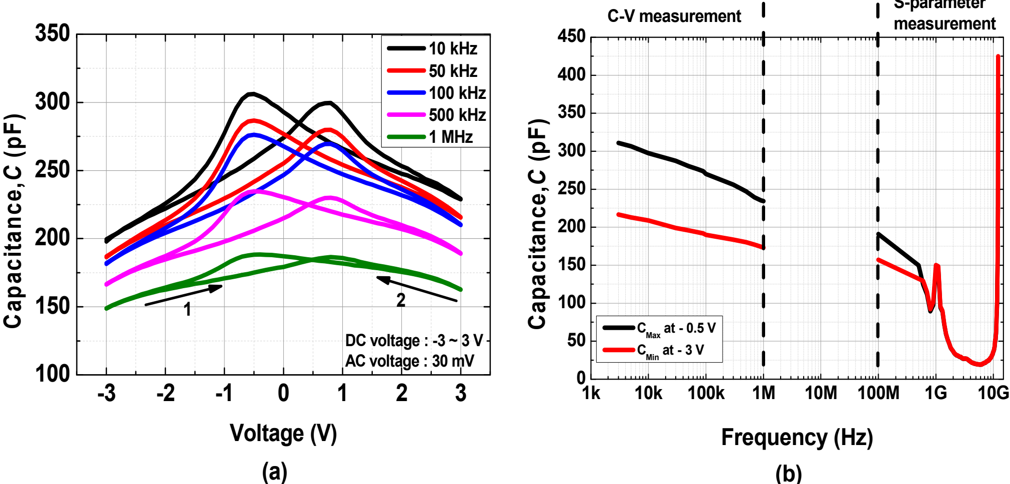

Figure 6. (**a**) Capacitance characteristics measured from 10 kHz to 1 MHz and (**b**) capacitance tunability characteristics versus frequency.

The C_{MAX} and C_{MIN} values extracted from the C–V and s-parameter measurements are plotted as functions of frequency in Figure 5b. Both the C_{MAX} and C_{MIN} values decreased as the frequency increased, reducing the capacitance tunability. Nevertheless, a capacitance tunability of up to several hundred MHz was achieved in this work. It is inferred that fabricated TiN/undoped HfO_2/TiN MFM capacitor can be utilized as a variable capacitor up to hundreds of MHz, which can be used to explore a new field of undoped HfO_2 MFM capacitors in microwave applications [41]. It is speculated that the rapid increase in capacitance at frequencies near 10 GHz is attributed to the series LC resonance.

4. Conclusions

In this study, the ferroelectric properties of TiN/undoped HfO_2/TiN MFM capacitors were evaluated over a wide range of temperatures and frequencies. A 10 nm thick undoped HfO_2 film was deposited via ALD, which was annealed at 650 °C after forming the electrodes. The fabricated MFM capacitor exhibited stable ferroelectric properties up to 150 °C with negligible degradation. Although the ferroelectric property weakened at temperatures higher than 200 °C, the hysteresis characteristics were maintained up to ~300 °C, which is the highest temperature reported for ferroelectric films. The frequency limitation was examined using C–V and s-parameter measurements, from which the capacitance tunability was achieved up to several hundred MHz. This study reveals the ultimate application conditions for a ferroelectric undoped HfO_2 MFM capacitor.

Author Contributions: Device fabrication, data curation, visualization, and writing—original draft preparation, C.-H.J.; formal analysis and validation, H.-S.K.; review and editing, H.K.; resources, supervision, project administration, conceptualization, writing—review and editing, and funding acquisition, H.-Y.C.; All authors have read and agreed to the published version of the manuscript.

Funding: This work was supported by the Civil–Military Technology Cooperation Program (17-CM-MA-03), the Basic Science Research Program (2015R1A6A1A03031833, 2022R1A2C1003723).

Institutional Review Board Statement: Not applicable.

Informed Consent Statement: Not applicable.

Data Availability Statement: Not applicable.

Conflicts of Interest: The authors declare no conflict of interest.

References

1. Li, S.; Zhou, D.; Shi, Z.; Hoffmann, M.; Mikolajick, T.; Schroeder, U. Involvement of unsaturated switching in the endurance cycling of Si-doped HfO_2 ferroelectric thin films. *Adv. Electron. Mater.* **2020**, *6*, 2000264. [CrossRef]
2. Kim, H.J.; An, Y.; Jung, Y.C.; Mohan, J.; Yoo, J.G.; Kim, Y.I.; Hernandez-Arriaga, H.; Kim, H.S.; Kim, J.; Kim, S.J. Low-thermal-budget fluorite-structure ferroelectrics for future electronic device applications. *Phys. Status Solidi* **2021**, *15*, 2100028.
3. Bhargavi, G.N.; Khare, A.; Badapanda, T.; Anwar, M.S.; Brahme, N. Analysis of temperature and frequency dependent dielectric properties, dynamic hysteresis loop and thermal energy conversion in $BaZr_{0.05}Ti_{0.95}O_3$ ceramic. *J. Mater. Sci. Mater. Electron.* **2018**, *29*, 11439–11448. [CrossRef]
4. Fan, Z.; Chen, J.; Wang, J. Ferroelectric HfO_2-based materials for next-generation ferroelectric memories. *J. Adv. Dielectr.* **2016**, *6*, 1630003. [CrossRef]
5. Kim, S.J.; Mohan, M.J.; Summerfelt, S.R.; Kim, J. Ferroelectric $Hf_{0.5}Zr_{0.5}O_2$ thin films: A review of recent advances. *JOM* **2019**, *71*, 246–255. [CrossRef]
6. Jo, J.; Choi, W.Y.; Park, J.D.; Shim, J.W.; Yu, H.Y.; Shin, C. Negative capacitance in organic/ferroelectric capacitor to implement steep switching MOS devices. *Nano Lett.* **2015**, *15*, 4553. [CrossRef] [PubMed]
7. Khan, A.I.; Chatterjee, K.; Wang, B.; Drapcho, S.; You, L.; Serrao, C.; Bakaul, S.R.; Ramesh, R.; Salahuddin, S. Negative capacitance in a ferroelectric capacitor. *Nat. Mater.* **2015**, *14*, 182–186. [CrossRef] [PubMed]
8. Gene, H. Haertling. Ferroelectric ceramics: History and technology. *J. Am. Ceram. Soc.* **1999**, *82*, 797.
9. Park, M.H.; Lee, Y.H.; Kim, H.J.; Kim, Y.J.; Moon, T.; Kim, K.D.; Müller, J.; Kersch, A.; Schroeder, U.; Mikolajick, T.; et al. Ferroelectricity and antiferroelectricity of doped thin HfO_2-based films. *Adv. Mater.* **2015**, *27*, 1811. [CrossRef] [PubMed]
10. Cheynet, M.C.; Pokrant, S.; Tichelaar, F.D.; Rouvière, J.-L. Crystal structure and band gap determination of HfO_2 thin films. *J. Appl. Phys.* **2007**, *101*, 054101. [CrossRef]
11. Bae, K.; Do, S.; Lee, J.; Lee, Y. Electrical and material characteristics of HfO_2 film in HfO_2/Hf/Si MOS structure. *J. Korean Inst. Electr. Electron. Mater. Eng.* **2009**, *22*, 101–106.
12. Kim, K.D.; Park, M.H.; Kim, H.J.; Kim, Y.J.; Moon, T.; Lee, Y.H.; Hyun, S.D.; Gwon, T.; Hwang, C.S. Ferroelectricity in undoped-HfO_2 thin films induced by deposition temperature control during atomic layer deposition. *J. Mater. Chem. C* **2016**, *4*, 6864–6872. [CrossRef]
13. Kwon, Y.; Lee, M.; Oh, J. Deposition and electrical properties of Al_2O_3 and HfO_2 films deposited by a new technique of proximity-scan ALD (PS-ALD). *Korean J. Mater. Res.* **2008**, *18*, 148–152. [CrossRef]
14. Gaskins, J.T.; Hopkins, P.E.; Merrill, D.R.; Bauers, S.R.; Hadland, E.; Johnson, D.C.; Koh, D.; Yum, J.H.; Banerjee, S.; Nordell, B.J.; et al. Review—Investigation and review of the thermal, mechanical, electrical, optical, and structural properties of atomic layer deposited high-k dielectrics: Beryllium oxide, aluminum oxide, hafnium oxide, and aluminum nitride. *ECS J. Solid State Sci. Technol.* **2017**, *6*, N189. [CrossRef]
15. Jang, Y.; Lee, S.M.; Jung, D.H.; Yum, J.H.; Larsen, E.S.; Bielawski, C.W.; Oh, J. Improved dielectric properties of BeO thin films grown by plasma enhanced atomic layer deposition. *Solid-State Electron.* **2020**, *163*, 107661. [CrossRef]
16. Müller, J.; Polakowski, P.; Riedel, S.; Mueller, S.; Yurchuk, E.; Mikolajick, T. Ferroelectric hafnium oxide A game changer to FRAM? In Proceedings of the 14th Annual Non-Volatile Memory Technology Symposium (NVMTS), Jeju, Korea, 27–29 October 2014.
17. Yin, Y.; Shen, Y.; Wang, H.; Chen, X.; Shao, L.; Hua, W.; Wang, J.; Cui, Y. In situ growth and characterization of TiN/$Hf_xZr_{1-x}O_2$/TiN ferroelectric capacitors. *Acta Phys. Chim. Sin.* **2022**, *38*, 2006016.
18. Shin, W.; Bae, J.H.; Kim, S.; Lee, K.; Kwon, D.; Park, B.G.; Kwon, D.; Lee, J.H. Effects of high-pressure annealing on the low-frequency noise characteristics in ferroelectric FET. *IEEE Electron. Device Lett.* **2022**, *43*, 13–16. [CrossRef]
19. Bae, J.H.; Kwon, D.; Jeon, N.; Cheema, S.; Tan, A.J.; Hu, C.; Salahuddin, S. Highly Scaled, High Endurance, Ω-Gate, Nanowire Ferroelectric FET Memory Transistors. *IEEE Electron. Device Lett.* **2020**, *41*, 1637–1640. [CrossRef]
20. Awadhiya, B.; Kondekar, P.N.; Meshram, D.M. Investigating Undoped HfO_2 as Ferroelectric Oxide in Leaky and Non-Leaky FE–DE Heterostructure. *Trans. Electr. Electron. Mater.* **2019**, *20*, 467–472. [CrossRef]
21. Polakowski, P.; Muller, J. Ferroelectricity in undoped hafnium oxide. *Appl. Phys. Lett.* **2015**, *106*, 232905. [CrossRef]

22. Pa, A.; Narasimhan, V.K.; Weeks, S.; Littau, K.; Pramanik, D.; Chiang, T. Enhancing ferroelectricity in dopant-free hafnium oxide. *Appl. Phys. Lett.* **2017**, *110*, 022903.
23. Kim, G.M.; Ohmi, S.-i. Ferroelectric properties of undoped HfO_2 directly deposited on Si substrates by RF magnetron sputtering. *Jpn. J. Appl. Phys.* **2018**, *57*, 11UF09. [CrossRef]
24. Kim, K.D.; Lee, Y.H.; Gwon, T.h.; Kim, Y.J.; Kim, H.J.; Moon, T.h.; Hyun, S.D.; Park, H.W.; Park, M.H.; Hwang, C.S. Scale-up and optimization of HfO_2-ZrO_2 solid solution thin films for the electrostatic supercapacitors. *Nano Energy* **2017**, *39*, 390–399. [CrossRef]
25. Han, S.; Lee, C.; Lee, J.; Cha, H. Study on the ferroelectric properties of ALD-HfO_2 in microwave band for tunable RF apparatus. j. inst. *Korean Electr. Electron. Eng.* **2018**, *22*, 780–785.
26. Nishimura, T.; Xu, L.; Shibayama, S.; Yajima, T.; Migita, S.; Toriumi, A. Ferroelectricity of nondoped thin HfO_2 films in TiN/HfO_2/TiN stacks. *Jpn. J. Appl. Phys.* **2016**, *55*, 08PB01. [CrossRef]
27. Han, S.; Lee, C.; Shin, H.; Lee, J.; Cha, H. Investigation of frequency-dependent permittivity tenability of P(VDF−TrFE) metal-ferroelectric-metal capacitor. *Results Phys.* **2019**, *12*, 469–470. [CrossRef]
28. Chen, H.; Tang, L.; Liu, L.; Chen, Y.; Luo, H.; Yuan, X.; Zhang, D. Temperature dependent polarization-switching behavior in $Hf_{0.5}Zr_{0.5}O_2$ ferroelectric film. *Materialia* **2020**, *14*, 100919. [CrossRef]
29. Zhang, Y.; Chen, Z.; Cao, W.; Zhang, Z. Temperature and frequency dependence of the coercive field of $0.71PbMb_{1/3}Nb_{2/3}O_3$–$0.29PbTiO_3$ relaxor-based ferroelectric single crystal. *Appl. Phys. Lett.* **2017**, *111*, 172902. [CrossRef]
30. Qiao, H.; He, C.; Wang, Z.; Pang, D.; Li, X.; Liu, Y.; Long, X. Influence of Mn dopants on the electrical properties of $Pb(In_{0.5}Nb_{0.5})O_3$–$PbTiO_3$ ferroelectric single crystals. *RSC Adv.* **2017**, *7*, 32607. [CrossRef]
31. Chen, X.; Qiao, X.; Zhang, L.; Zhang, J.; Zhang, Q.; He, J.; Mu, J.; Hou, X.; Chou, X.; Geng, W. Temperature dependence of ferroelectricity and domain switching behavior in $Pb(Zr_{0.3}Ti_{0.7})O_3$ ferroelectric thin films. *Ceram. Int.* **2019**, *45*, 18030. [CrossRef]
32. Saif, A.A.; Saif, Z.A.Z.; Jamal, Z.S.; Poopalan, P. Frequency dependent electrical properties of ferroelectric $Ba_{0.8}Sr_{0.2}TiO_3$ Thin Film. *Mater. Sci.* **2011**, *17*, 2. [CrossRef]
33. Lee, D.H.; Yang, K.; Park, J.Y.; Park, M.H. A brief review on the effect of impurities on the atomic layer deposited fluorite-structure ferroelectrics. *J. Korean Inst. Surf. Eng.* **2020**, *53*, 169–181.
34. Valipour, M.; Aman, M.; Singh, M.R. Rawat. Increasing of hardness of titanium using energetic nitrogen ions from sahand as a filippov type plasma focus facility. *J. Fusion Energ.* **2012**, *31*, 65–72. [CrossRef]
35. Suzuki, K.; Imasaki, K.; Ito, Y.; Miura, H. Strain dependence of dielectric properties and reliability of high-k thin films. In Proceedings of the International Conference on Simulation of Semiconductor Processes and Devices, San Diego, CA, USA, 9–11 September 2009.
36. Antons, A.; Neaton, J.B.; Rabe, K.M.; Vanderbilt, D. Tunability of the dielectric response of epitaxially strained $SrTiO_3$ from first principles. *Phys. Rev. B* **2005**, *71*, 024102. [CrossRef]
37. Wang, J.; Wang, D.; Li, Q.; Zhang, A.; Gao, D.; Guo, M.; Feng, J.; Fan, Z.; Chen, D.; Qin, M.; et al. Excellent ferroelectric properties of $Hf_{0.5}Zr_{0.5}O_2$ thin films induced by Al_2O_3 dielectric layer. *IEEE Electron. Device Lett.* **2019**, *40*, 1937–1940. [CrossRef]
38. Liu, Y.; Aziguli, H.; Zhang, B.; Xu, W.; Lu, W.; Bernholc, J.; Wang, Q. Ferroelectric polymers exhibiting behaviour reminiscent of a morphotropic phase boundary. *Nature* **2018**, *562*, 96–100. [CrossRef] [PubMed]
39. Harrington, S.A.; Zhai, J.; Denev, S.; Gopalan, V.; Wang, H.; Bi, Z.; Redfern, S.A.T.; Baek, S.H.; Bark, C.W.; Eom, C.B.; et al. Thick lead-free ferroelectric films with high Curie temperatures through nanocomposite-induced strain. *Nat. Nanotechnol.* **2011**, *6*, 491–495. [CrossRef] [PubMed]
40. Pozar, D.M. *Microwave Engineering*; John Wiley & Sons: Hoboken, NJ, USA, 2021.
41. Ren, Y.; Huang, Z.; Guo, L.-F. A electrically tunable patch antenna with P(VDF-TrFE) thin film. In *Material Engineering and Mechanical Engineering (MEME2015)*; World Scientific: Hangzhou, China, 2015; pp. 239–245.